

論文の内容の要旨

Photoelectron–ion correlation created by photoionization of H₂ and correlated molecule–photon dynamics in a cavity

(H₂の光イオン化によって生成する
光電子–イオン相関と
共振器中の分子–光子の相関動力学)

氏名 西 孝哲

1. Introduction

When an atom or a molecule is irradiated with an ultrashort laser pulse, photoionization can proceed. Upon the photoionization, a correlated pair of an ion and a photoelectron is produced. If the ion has one or more than one electrons and/or the ion is composed of more than one nuclei, coherent motions of the constituent particles are created within the ion, and the coherent motions carry the information on the photoelectron because the ion and the photoelectron are correlated.

It has been known that the coherent motion of an ion created upon photoionization of an atom by the irradiation of an ultrashort pulse can be characterized by a reduced matrix ρ_{ion} of the created ion [1]. However, it has not been explored yet how the correlation between a photoelectron and an ion is encoded in the reduced matrix of the ion. In order to understand how the correlation between a photoelectron and an ion produces the coherence in the ion, I investigate theoretically photoionization of H₂ by an ultrashort XUV laser pulse, and describe the coherent vibrational motion of H₂⁺ by its reduced density matrix ρ_{vib} .

First, I introduce a concept of entanglement, which can be defined unambiguously for a bipartite system, to discuss quantitatively how the extent of the correlation is influenced by the parameters of the XUV laser pulse such as its wavelength, pulse duration, and field intensity.

Next, in order to evaluate the effect of the correlation on the coherent vibrational motion of H₂⁺, I calculate the phase of the reduced density matrix ρ_{vib} . When we discuss the phase of the reduced density matrix of the ion, we need to know not only the initial phase transferred from the phase of the laser pulse and the dynamical phase originating from the field-free evolution of the ion but also the phase of the photoelectron wave function originating from the interaction between the ion and the photoelectron. However, to the best of our knowledge, the phase of the photoelectron wave function has not been explicitly considered before in the determination of the reduced density matrix. In the thesis, I determine the phase of ρ_{vib} by evaluating the phase of the photoelectron wave function.

On the other hand, when a photon is emitted from an atom or from a molecule placed in a cavity, the photon and the atom or molecule are correlated with each other. In recent years, the molecule–photon coupling in a cavity has been attracting attention for its potential applications in quantum information as well as for its capability of controlling chemical reactions [2, 3]. It has been known that a correlation between a photon and a molecule can be investigated for a model system in which a molecule is trapped in a plasmonic nanocavity [2]. I investigate in the thesis the correlated dynamics of a molecule

and a photon in a cavity and develop a numerical algorithm to simulate a photon emission from the cavity.

2. Entanglement between H_2^+ and e^-

After the photoionization of H_2 , the total system, $\text{H}_2^+ + e^-$, is described by the wave packet,

$$|\Phi\rangle = \sum_{\nu} \int d\mathbf{k}_e a_{\nu\mathbf{k}_e} |\chi_{\nu}\phi_{1s}\rangle |\psi_{\mathbf{k}_e}\rangle, \quad (1)$$

where $|\chi_{\nu}\rangle$ and $|\phi_{1s}\rangle$ are the vibrational and electronic eigenfunctions of $\text{H}_2^+(1s\sigma_g)$, respectively, ν is the vibrational quantum number, $|\psi_{\mathbf{k}_e}\rangle$ is the photoelectron energy eigenfunction, \mathbf{k}_e is the photoelectron momentum, and $a_{\nu\mathbf{k}_e}$ is the transition amplitude from the ground state of H_2 to the final state $|\chi_{\nu}\phi_{1s}\rangle |\psi_{\mathbf{k}_e}\rangle$. In order to quantify the correlation between H_2^+ and e^- using the entanglement between these two particles, I calculate the reduced density matrix of either H_2^+ or e^- , and we adopt that of H_2^+ ,

$$\rho_{\text{vib}} = \sum_{\nu\nu'} \int d\mathbf{k}_e a_{\nu\mathbf{k}_e} a_{\nu'\mathbf{k}_e}^* |\chi_{\nu}\rangle \langle\chi_{\nu'}|, \quad (2)$$

which represents the vibrational coherence of H_2^+ . As a quantifier of the extent of entanglement, I choose the purity of the reduced density matrix because it is directly related to the coherence of the subsystem, i.e., H_2^+ in this case. The purity P is defined as the trace of ρ_{vib}^2 as

$$P = \text{Tr}[\rho_{\text{vib}}^2] = \sum_{\nu\nu'} \left| \int d\mathbf{k}_e a_{\nu\mathbf{k}_e} a_{\nu'\mathbf{k}_e}^* \right|^2. \quad (3)$$

The purity becomes 1, i.e., $P = 1$, when H_2^+ and e^- are not entangled while it decreases as the extent of entanglement between H_2^+ and e^- increases.

I adopt the one-dimensional model, in which the electrons and the protons move along the direction of the electric field of the linearly polarized light, and solve the time-dependent Schrödinger equation using the grid method. In Fig. 1, the purities calculated using seven different sets of laser parameters are plotted. As shown in this figure, the purity decreases as the pulse duration increases and does not vary sensitively to the wavelength and the peak intensity. Because the spectral bandwidth decreases as the pulse duration increases, it becomes possible to determine the vibrational state of H_2^+ only by measuring the energy of the photoelectron ω_k . In other words, as the pulse duration increases, the photoelectron carries more information on the vibrational state of H_2^+ , and the extent of the entanglement between the photoelectron and H_2^+ becomes larger.

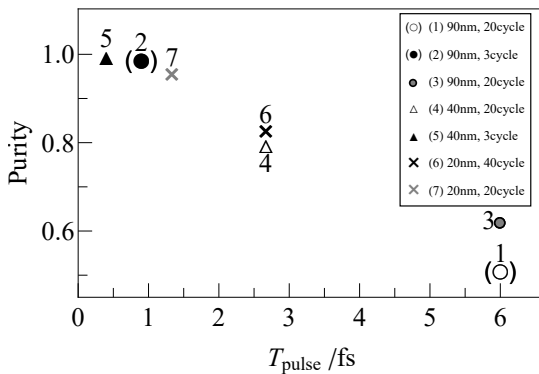


FIG. 1. The purity as a function of the pulse duration for the seven different sets of laser parameters. The intensity is set to 10^{15} Wcm^{-2} except (1) and (2), for which the intensity is set to 10^{13} Wcm^{-2} .

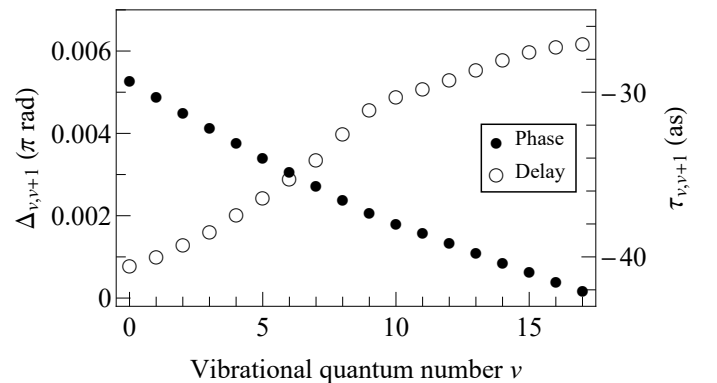


FIG. 2. The intrinsic phase of the reduced density matrix between ν th state and $(\nu + 1)$ th state, $\Delta_{\nu, \nu+1}$, and the corresponding intrinsic time delay, $\tau_{\nu, \nu+1}$.

3. Time delay in the vibrational motion of H_2^+

When H_2^+ created by the photoionization is irradiated with a probe pulse so that H_2^+ dissociates into $H + H^+$, the kinetic energy release (KER) of H^+ , is known to oscillate as a function of the pump–probe time delay τ [4]. This oscillation can be characterized not only by the dynamical phase, $-\omega_{v,v'}\tau \equiv -(\omega_v - \omega_{v'})\tau$, but also by a phase intrinsic to the ionization process. This intrinsic phase is related to the phase of the reduced density matrix as

$$\Delta_{v,v'} = \arg[(\rho_{\text{vib}}(\tau))_{v,v'}] - (-\omega_{v,v'}\tau) = \arg \left[\int d\mathbf{k}_e a_{v\mathbf{k}_e} a_{v'\mathbf{k}_e}^* \right] - (-\omega_{v,v'}\tau). \quad (4)$$

From the variation of the KER in τ , which is called the delay–KER spectrogram, the intrinsic delay, $\tau_{v,v'}$, defined using the intrinsic phase as $\tau_{v,v'} = \Delta_{v,v'}/\omega_{v,v'}$, can be extracted.

I calculate the transition amplitude of the ionization process using the first-order perturbation theory and derive $\Delta_{v,v'}$ and $\tau_{v,v'}$. In order to describe the phase created by the ionization process precisely, I express the photoelectron wave function using the two-center Coulomb wave function. As an ionization laser pulse, I adopt an attosecond pulse train, by which an experimental delay–KER spectrogram of H_2^+ was recorded recently [4].

In Fig. 2, the intrinsic phase and the intrinsic time delay between v th and $(v+1)$ th vibrational levels of H_2^+ are plotted. The intrinsic phases are found to be of the order of $10^{-3}\pi$ radian, and consequently, the corresponding time delay is in the range between -43 as -27 as. The complex phase of the photoelectron wave function, which is determined by the phase shift originating from the Coulombic potential created by H_2^+ , depends only weakly on v . Because only the photoelectron wave function $\psi_{\mathbf{k}_e}$ is the complex-valued function appearing in the calculation of the amplitude of the transition $a_{v\mathbf{k}_e}$ from the ground state of H_2 , $|\Psi_0\rangle$, to the final state, $|\chi_v \phi_{1s} \psi_{\mathbf{k}_e}\rangle$, the phase of $a_{v\mathbf{k}_e}$ also weakly depends on v . Consequently, the phase differences, $\arg[a_{v\mathbf{k}_e}] - \arg[a_{v+1,\mathbf{k}_e}]$, becomes of the order of tens of attoseconds. In order to extract the intrinsic delay $\tau_{v,v+1}$ from the delay–KER spectrogram, the pump–probe time delay τ should be measured with precision of the order of $\tau_{v,v+1}$, which is as small as 27 as. Considering the uncertainty of the pump–probe time delay in Ref. [4] was about 80 as, the required uncertainty of 27 as can be within range of future experiments.

4. Correlated molecule–photon dynamics

In order to study the coupled molecule–photon dynamics in a cavity, I choose a model system composed of a molecule having two vibronic modes and a cavity having only one mode. I assume that the potential energy curves of two electronic states, $|g\rangle$ and $|e\rangle$, are modeled by harmonic oscillators, and the cavity is pumped by the continuous wave laser whose frequency is resonant with the cavity mode. The coupling between the electronic excitation and the cavity excitation is described through the vacuum Rabi frequency Ω_0 . I assume the spontaneous emission from the molecule into the vacuum is negligible compared with the decay of the cavity photon.

I numerically integrate the master equation,

$$\dot{\rho} = -i[H, \rho] - \gamma/2 (a^\dagger a \rho + \rho a^\dagger a) + a \rho a^\dagger, \quad (5)$$

where ρ is the density matrix of the molecule–photon system, H is the Hamiltonian of the coupled molecule–photon system, and a is the annihilation operator of the cavity photon whose decay rate is γ .

In order to efficiently simulate the vibrational motion of the molecule in the cavity, I also solve the master equation by using the Monte Carlo wave packet (MCWP) method [5], with which we can express the system by the state vector instead of the density matrix, so that we can reduce the computational cost significantly. In the MCWP method, the state vector of the system, $|\Psi\rangle$, is propagated under the non-Hermitian Hamiltonian, $H_{\text{NH}} = H - i\gamma/2 a^\dagger a$, and then, the decrease in the norm, dp , during the time propagation from t to $t + dt$, is calculated. Finally, in order to mimic the randomness of the photon detection in the experiment, a random number ϵ is chosen at each time step, and the annihilation operator a is

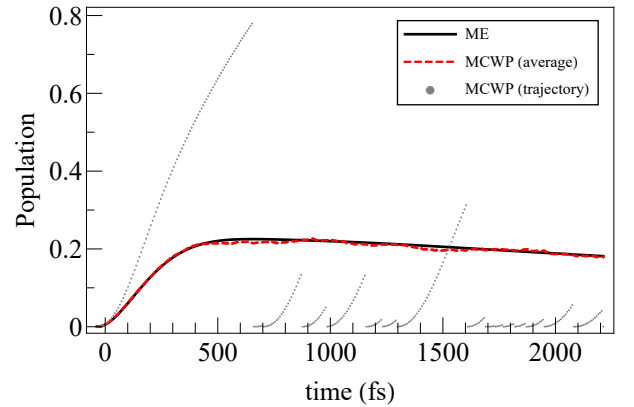


FIG. 3. The population of the electronic excited state $|e\rangle$ calculated by the numerical integration of the master equation (ME, solid line) and by the MCWP method (MCWP(average), dashed line). A trajectory (dots) shows abrupt damping at random times, which corresponds to the detection of the photon emitted from the cavity.

applied to the state vector if $\epsilon < dp$ is satisfied at t , which means the photon is detected at t . We call each state vector $|\Psi\rangle$ the trajectory and, by averaging over a large number N of trajectories, we can obtain the density matrix $\rho = 1/N \sum_j^N |\Psi_j\rangle \langle \Psi_j|$ equivalent to that obtained by the numerical integration of the master equation.

In Fig. 3, the population of the electronic excited state $|e\rangle$ with $\Omega_0 = \gamma/10$ obtained by the numerical integration of the master equation (solid line) shows the damped Rabi oscillation, which is well reproduced by using the MCWP method by averaging over 4000 trajectories (dashed line). A trajectory of the MCWP method, $|\Psi\rangle$ (dots), shows the Rabi oscillation and discontinuities at random times, at which the condition $\epsilon < dp$ is satisfied, i.e., the photon is detected. As the trajectory shown in Fig. 3 indicates, photon detection occurs frequently because γ is large compared with Ω_0 .

Because the cavity excited state evolves much faster than the molecular ground and excited states when $\Omega_0 < \gamma$, we have eliminated the cavity mode and developed an effective operator method [6], which describes the system within a compact Hilbert space and give insights into the dynamics. We have confirmed that the effective operator method reproduces the exact results obtained with the original master equation. By combining the effective operator method with the MCWP method, we have clarified that the photon emission explicitly depends on the nuclear position and the coherence between the vibronic states.

-
- [1] E. Goulielmakis, Z.-H. Loh, A. Wirth, R. Santra, N. Rohringer, V. S. Yakovlev, S. Zherebtsov, T. Pfeifer, A. M. Azzeer, M. F. Kling, S. R. Leone, and F. Krausz, *Nature* **466**, 739 (2010).
 - [2] R. Chikkaraddy, B. de Nijs, F. Benz, S. J. Barrow, O. A. Scherman, E. Rosta, A. Demetriadou, P. Fox, O. Hess, and J. J. Baumberg, *Nature* **535**, 127 (2016).
 - [3] J. Galego, F. J. Garcia-Vidal, and J. Feist, *Physical Review Letters* **119**, 136001 (2017).
 - [4] Y. Nabekawa, Y. Furukawa, T. Okino, A. A. Eilanlou, E. J. Takahashi, K. Yamanouchi, and K. Midorikawa, *Nature communications* **6**, 8197 (2015).
 - [5] J. Dalibard, Y. Castin, and K. Mølmer, *Physical Review Letters* **68**, 580 (1992).
 - [6] F. Reiter and A. S. Sørensen, *Physical Review A* **85**, 032111 (2012).